

Pre-reionization Fossils, Ultra-faint Dwarfs and the Missing Galactic Satellite Problem

Mia S. Bovill and Massimo Ricotti

Department of Astronomy, University of Maryland, College Park, MD 20742

msbovill@astro.umd.edu, ricotti@astro.umd.edu

ABSTRACT

We argue that, at least a fraction of the newly discovered population of ultra-faint dwarf spheroidal galaxies in the Local Group constitute the fossil relic of a once ubiquitous population of dwarf galaxies formed before reionization with circular velocities smaller than $v_c^{cr} \sim 20$ km/s. We present several arguments in support of this model. The number of luminous Milky Way satellites inferred from observations is larger than the estimated number of dark halos in the Galaxy that have, or had in the past, a circular velocity $> v_c^{cr}$, as predicted by the “Via Lactea” simulation. This implies that some ultra-faint dwarfs are fossils. However, this argument is weakened by recent results from the “Aquarius” simulations showing that the number of Galactic dark matter satellites is 2.5 larger than previously believed. Secondly, the existence of a population of ultra-faint dwarfs was predicted by cosmological simulations in which star formation in the first minihalos is reduced – but not suppressed – by radiative feedback. Here, we show the statistical properties of the fossil galaxies in those simulations are consistent with observations of the new dwarf population and with the number and radial distribution of Milky Way satellites as a function of their luminosity. Finally, the observed Galactocentric distribution of dwarfs is consistent with a fraction of dSphs being fossils. To make our case more compelling, future work should determine whether stellar chemical abundances of simulated “fossils” can reproduce observations and whether the tidal scenarios for the formation of Local Group dwarf spheroidals are equally consistent with all available observations.

Subject headings: cosmology: theory — galaxies: formation — stars: formation

1. Introduction

Hierarchical formation scenarios predict that most of the galactic halos that formed before reionization (at $z = 6 - 10$) had masses below $10^8 - 10^9 M_\odot$. Those that survived to the modern epoch, if they were able to form stars, would constitute a sub-population of dwarf satellites orbiting larger halos. N-body simulations of cold dark matter (CDM) predict a number of dark matter

halos around the Milky Way and M31 that is much greater than the number of observed luminous satellites (Klypin et al. 1999; Moore et al. 1999). This may indicate a problem with the CDM paradigm or that feedback processes are very efficient in suppressing star formation in the first small mass halos, which remain mostly dark. Recent observational and theoretical advances require a re-visitation of the missing galactic satellite problem. In addition, cosmological simulations of the formation of the first galaxies have shown most previously known dwarf spheroidals (dSphs) to have properties consistent with the surviving first galaxies, and predicted the existence of an undiscovered, lower surface brightness population of dwarfs (Ricotti & Gnedin 2005) (hereafter, RG05). The recent discovery of a population of ultra-faint dwarfs confirms the aforementioned theoretical expectation and allows us to test in great detail cosmological simulations of the first galaxies, addressing important theoretical questions on feedback in the early universe and on the nature of dark matter.

The formation of the first dwarf galaxies - before reionization - is regulated by complex feedback effects that act on cosmological scales. These self-regulation mechanisms have dramatic effects on the number and luminosity of the first, small mass galaxies, and yet, are unimportant for the formation of galaxies more massive than $10^8 M_\odot$, that may form before and after reionization. Galaxy formation in the high redshift universe is peculiar due to (i) the lack of important coolants, such as carbon and oxygen, in a gas of primordial composition and (ii) the small typical masses of the first dark halos. The gas in halos with circular velocity smaller than 20 km s^{-1} (roughly corresponding to a mass $M \lesssim 10^8 M_\odot$ at the typical redshift of virialization) is heated to temperatures $\lesssim 10,000 \text{ K}$ during virialization. At this temperature, a gas of primordial composition is unable to cool and initiate star formation unless it can form a sufficient amount of H_2 ($x_{\text{H}_2} \gtrsim 10^{-4}$). Although molecular hydrogen is easily destroyed by far ultraviolet (FUV) radiation (negative feedback), its formation can be promoted by hydrogen ionizing radiation emitted by massive stars, through the formation of H^- (positive feedback) (Haiman et al. 1996).

It is difficult to determine the net effect of radiative feedback on the global star formation history of the universe before the redshift of reionization. The effect of a dominant FUV background (at energies between 11.34 eV and 13.6 eV) is to destroy H_2 , the primary coolant at the start of galaxy formation. The FUV radiation emitted by the first few Population III stars is sufficient to suppress or delay galaxy formation in halos with circular velocities $v_c < v_c^{cr} \sim 20 \text{ km s}^{-1}$. According to this scenario, most halos with masses $< 10^8 - 10^9 M_\odot$ do not form stars and remain dark. Therefore, the number of pre-reionization fossils in the Local Group would be expected to be very small or zero. However, this model does not take into account the effect of ionizing radiation and “positive feedback regions” (Ricotti et al. 2001; Ahn et al. 2006; Whalen et al. 2008), that may have a dominant role in regulating galaxy formation before reionization (Ricotti et al. 2002a,b). Simulations including these processes show that star formation in the first small mass halos is inefficient, mainly due to winds produced by internal UV sources. This produces galaxies that are extremely faint and have very low surface brightnesses. However, according to the results of our simulations, a large number of these ultra-faint dwarfs (a few hundred galaxies per co-moving

Mpc³) form before reionization at $z \sim 7 - 10$. Hence, according to this model, the Local Volume and the Local Group should contain hundreds of ultra-faint dwarf galaxies.

The small masses of the first minihalos have two other implications. First, the ionizing radiation emitted by massive stars can blow out most of the gas before SN-driven winds become important, further reducing star formation rates (Ricotti et al. 2008). Second, the increase in temperature of the intergalactic medium (IGM) to 10,000 – 20,000 K due to H I reionization, prevents the gas from condensing into newly virialized halos with circular velocities smaller than 10 – 20 km s⁻¹, with a critical value that depends on redshift (Gnedin 2000; Okamoto et al. 2008). It follows, that dwarf galaxies with $v_c < 10 - 20$ km s⁻¹ stop forming stars after reionization. However, the value $v_c^{cr} \sim 20$ km s⁻¹ that we use to define a fossil is primarily motivated by the fundamental differences discussed above in cooling and feedback processes that regulate star formation in the early Universe and is not the critical value for suppression of star formation due to reionization. Indeed, Ricotti (2009) argues that fossils dwarfs can have a late phase of gas accretion and star formation well after reionization, at redshift $z < 1 - 2$. Thus, a complete suppression of star formation after reionization (about 12 Gyr ago) is not a defining property of a fossil dwarf.

Data on the velocity dispersion of the stars, σ , the only observational measure of halo mass, shows that a typical dSph has $\sigma < 20$ km s⁻¹. However, the circular velocity of the dark halo can be much larger than σ if typical radius of the stellar spheroid is much smaller than the dark halo radius. For a pre-reionization fossil, according to simulations in RG05, on average we measure $\sigma/v_c \sim 0.5$ at formation (see Fig. 2 in RG05).

RG05 compared the statistical properties of simulated pre-reionization galaxies to observations of Local Group dwarfs available in 2004-2005. Based on similarities between observed dSphs and simulated galaxies formed before reionization, they argued that many dSphs may be “fossils” of the first galaxies. RG05 also predicted the existence of a yet undetected population of ultra-faint dSph galaxies. (Gnedin & Kravtsov 2006) (hereafter, GK06) used results from RG05 to predict the radial distribution of fossils around the Milky Way and their Galactocentric luminosity function. They found a good agreement of simulations with observations for the most luminous fossils but, again, a lack of observed ultra-faint fossils, mainly in the outer Milky Way halo. An ultra-faint population of dSphs has now been found in the Local Group. As we will show in the present work, these new dwarfs have properties in agreement with our simulations of pre-reionization fossils. This discovery is certainly one of the most exciting developments in understanding galaxy formation in the early universe and has drawn renewed attention to “near field cosmology” as a tool to understand galaxy formation. The new galaxies have been discovered by data mining the SDSS and surveys of the halo around M31, resulting in the discovery of 12 new ultra-faint Milky Way satellites (Belokurov et al. 2006, 2007; Irwin et al. 2007; Walsh et al. 2007; Willman et al. 2005b,a; Zucker et al. 2006b,a; Geha et al. 2009) and six new companions for M31 (Ibata et al. 2007; Majewski et al. 2007; Martin et al. 2006).

Here, we also argue that solely based on the observed number of Milky-Way satellites, at least a

few of them must be a pre-reionization fossil, that means: it must have formed before reionization in a halo with circular velocity < 20 km/s. However, some ultra-faint dwarfs may not be pre-reionization fossils. As we write, several works have been published that seem to show that the observed properties of the ultra-faint dwarf population can also be explained in the context of the tidal scenario, that assumes that these galaxies formed after reionization in halos that were much more massive and had different properties at the time of formation (Peñarrubia et al. 2008). It is intriguing that both the tidal scenario and the pre-reionization fossil scenario are able to produce a population of ultra-faint dwarfs that follow very similar statistical trends in terms of size, surface brightness, mass to light ration and metallicity-luminosity relation. The jury is still out.

This paper is laid out as follows. In § 2, we collect published data on the new dwarf population and, after correcting for completeness of the surveys, we estimate the total number of Local Group satellites (which increases from 32 to about 100). Using the results of published N-body simulations, we compare the observed number of luminous satellites to the estimated number of dark satellites that have or had in the past a circular velocity $> v_c^{cr}$, using the results of published N-body simulations, concluding that some ultra-faint dwarfs must be pre-reionization fossils. In § 3 we show that the properties of the new Milky Way and M31 dwarfs are in remarkable agreement with the theoretical data on the “fossils” from RG05 and with their Galactocentric distribution around the Milky Way calculated in GK06. In § 4 we discuss the implications of the new dwarfs on the formation of the first galaxies and the missing galactic satellite problem.

2. Data and Completeness Corrections

In Table 1, we summarize the observed properties of the new dwarfs. The new Milky Way satellites were discovered using SDSS Data Release 4 and 5 (Adelman-McCarthy et al. 2006, 2007). When multiple references are available for a dwarf property, we defer to the measurement with the smallest error bars. Excepting Bootes I and II, Canes Venatici I and Leo T, where central surface brightness measurements were available, the average surface brightness inside the half light radius, $r_{1/2}$, was used: $\Sigma_V = L_V / (2\pi r_{1/2}^2)$.

Recent surveys of M31 (Martin et al. 2006; Ibata et al. 2007) have covered approximately a quarter of the space around the M31 spiral. The survey have found 6 new M31 satellites. If we make a simple correction for the covered are of the survey we find that, including the new dwarfs, the estimated number of M31 satellites increases from 9 to 33 ± 10 . Two new M31 satellites, And XII and And XIV, have velocities near or above their host’s escape velocity (Chapman et al. 2007; Majewski et al. 2007). Both galaxies are classified as dwarf spheroidals and show a lack of H I gas, and both are likely on their first approach towards a massive halo. Kinematic data is not yet available on these two dwarfs to determine whether their circular velocities are below the 20 km s^{-1} threshold, however their currently known properties meet the RG05 criteria for fossils.

In estimating the completeness correction for the number of the Milky Way dwarfs, one should

also account for selection effects from the limiting surface brightness sensitivity of the Sloan of $\sim 30 \text{ mag arcsec}^{-2}$ (Koposov et al. 2008). The sensitivity limit is shown as a solid line in Figure 1. Identification of new satellites depends on the visibility of the horizontal branch in the color-magnitude diagram, which, for the typical luminosity of the new faint dwarfs ($M_V \approx -4$) drops below SDSS detection limits at Galactocentric distances beyond $\sim 200 - 250 \text{ kpc}$ (Koposov et al. 2008). Of the new Milky Way dwarfs, only Leo T is well beyond this distance threshold and nine of the eleven new Milky Way satellites are within 200 kpc. We make the most conservative estimate, by assuming that we have a complete sample of dwarfs within 200 kpc. Additional selection bias for the new dwarfs comes primarily from the limits of the SDSS coverage on the sky. To account for this, we apply the zero-th order correction of multiplying the number of new dwarfs by 5.15 (Tollerud et al. 2008). This correction assumes an isotropic distribution of satellites when observed from the Galactic center. With this simple assumptions we estimate that the number of Milky Way satellites with Galactocentric distance $< 200 \text{ kpc}$ is about 85 ± 14 , including the 29 previously know satellites. The error estimate is due to shot noise.

However, bright satellites of the Milky Way are distributed very anisotropically (Kroupa et al. 2005; Zentner et al. 2005), so the assumption of isotropy may not be a good one. In addition, the luminous satellites can be radially biased, so the abundance of the faintest satellites within 50 kpc may not be easily corrected to larger distances without prior knowledge of this bias. And, of course, satellites of different luminosity and surface brightness will have different completeness limits. These selection biases have been considered in detail in a recent paper by Tollerud et al. (2008). This study finds that there may be between 300 to 600 luminous satellites within the virial radius of the Milky Way. Their estimate for the number of luminous satellites within a Galactocentric distance of about 200 kpc is 120, that is slightly larger than our simple (and more conservative) estimate.

2.1. Number of non-fossil satellites in the Milky Way

In this section, we use the results of published N-body simulations to estimate the number of dark halos in the Milky Way that have, or had, a circular velocity $v_c > 20 \text{ km/s}$. By definition, dwarf galaxies formed in these dark halos are not pre-reionization fossils. If we find that the number of observed Milky Way satellites exceeds the estimated number of these massive halos we must conclude that at least a fraction of the observed Milky Way satellites are pre-reionization fossils. GK06 have estimated that pre-reionization fossils may constitute about 1/3 of Milky Way dwarfs, based on detailed comparisons between predicted and observed Galactocentric distributions of dwarf satellites.

It is clear that if we simply count the number of dark halos within the Milky Way virial radius with $v_c \gtrsim 20 \text{ km/s}$, their number is much smaller than the current number of observed luminous satellites. However, a significant fraction of dark halos that today have $v_c < 20 \text{ km/s}$ were once more massive, due to tidal tripping (Kravtsov et al. 2004) . If the stars in these halos survive

tidal stripping for as long as the dark matter, they may indeed account for a fraction or all of the newly discovered ultra-faint dwarfs. Kravtsov et al. (2004) favor the idea that tidal stripping of the dark matter halo does not affect the stellar properties of the dwarf galaxy. Thus, this model is qualitatively similar to our model for pre-reionization fossils, save a rescaling of the mass of the dark halos hosting the dwarfs.

However, it is also possible that tidally stripped halos lose their stars more rapidly than they lose their dark matter. Thus, they may quickly transform from luminous to dark halos. Such a behavior has been found by Peñarrubia et al. (2008). According to this scenario, tidally stripped dark halos may not account for the observed ultra-faint population. To summarize, if the number of dark halos that have or had in the past $v_c \gtrsim 20$ km/s is smaller than the number of luminous Milky Way satellites we may conclude that some dwarfs are fossils. Vice versa, if the number is larger, we cannot make any conclusive statement about the origin of Milky Way satellites.

High resolution N-body simulations of the Milky Way system give the number of dark halos in the Milky Way as a function of their circular velocity v_c at $z = 0$. The “Via Lactea” simulation by Diemand et al. (2007) finds:

$$N_{dm}(> v_c) = N_{dm,20} \left(\frac{v_c}{20 \text{ km/s}} \right)^{-\alpha}, \quad (1)$$

with $N_{dm,20} \approx 27.7$ and $\alpha \approx 3$. However, a recent work by Springel et al. (2008) (the Aquarius simulations) finds a factor 2.5 more satellites at any given v_c , *i.e.*, $N_{dm,20} \approx 69$ and $\alpha \approx 3.15$. Although the Aquarius simulations have higher resolution than the Via Lactea simulation, the large disagreement between the two works is due to a systematic difference, possibly related to the creation of the initial conditions, and it is not due to the improved resolution. Although the Aquarius simulation is likely correct, we will provide predictions for both simulations (we have become aware of the Aquarius simulation results, that are not published yet, after this work had been mostly completed.)

To determine the importance of tidal mass loss for satellites around the Milky Way we use results from Kravtsov et al. (2004). Figure 5 in Kravtsov et al. (2004) gives the fraction of halos, $f(v_c)$, that presently have circular velocity v_c , but some time in the past had a circular velocity $\leq v_c^{max} = 20$ km/s, where as $v_c^{max} \equiv \max(v_c(t))$. We approximate the Kravtsov et al. (2004) results for $f(v_c)$ with the power law $f(v_c) \approx (v_c/20 \text{ km s}^{-1})^\beta$, with $\beta \approx 3.7$. We then calculate the number of dark halos $N_{dm}(v_c^{max} > 20 \text{ km s}^{-1})$ analytically:

$$\begin{aligned} N_{dm}(v_c^{max} > 20 \text{ km s}^{-1}) &= N_{dm}(v_c(z=0) > 20 \text{ km s}^{-1}) + \int_{v_{c,min}}^{20 \text{ km/s}} dv \frac{dN}{dv} f(v) \\ &= N_{dm,20} \left[1 + \frac{\alpha}{\beta - \alpha} (1 - x_{min}^{\beta - \alpha}) \right] \approx 2.64 N_{dm,20} \end{aligned}$$

where $x_{min} = v_{min}/20$ km/s, and $v_{min} \gtrsim \langle \sigma_* \rangle \approx 10$ km s⁻¹ roughly equals the mean observed velocity dispersion of the stars, $\langle \sigma_* \rangle$, of ultra-faint dwarf satellites. The rationale for integrating

to v_{min} is that observed satellites are dark matter dominated and cannot be hosted in dark halos that have $v_c < \sigma_*$, unless σ_* is not a tracer for the dark matter content of the halo (*e.g.*, due to tidal heating).

Using the above equation, we find 73 ± 16 and 182 ± 40 halos with $N_{dm}(v_c^{max} > 20 \text{ km s}^{-1})$ within R_{vir} , for the Via Lactea and Aquarius simulations respectively. Both these numbers are smaller than the 300 – 1000 luminous Milky Way satellites estimated by Tollerud et al. (2008). Taken at face value, these numbers indicate that a fraction of Milky Way satellites are true pre-reionization fossils. However, the number of luminous satellites that exist within the Milky Way is highly uncertain beyond a distance from the Galactic center of 200 kpc.

Based on Figures 11 and 12 in Springel et al. (2008) and Figure 5 in Tollerud et al. (2008), we estimate that roughly half of the Milky Way satellites (within the virial radius R_{vir}) are < 200 kpc from the Galactic center. Therefore, within 200 kpc we estimate 36 ± 8 and 91 ± 20 dark halos with $N_{dm}(v_c^{max} > 20 \text{ km s}^{-1})$ for the Via Lactea and Aquarius simulations respectively. These numbers can be compared to our estimated number of luminous satellites with $d < 200$ kpc (85 ± 14 satellites) and to the estimate by Tollerud et al. (2008) (120 satellites). Using the Via Lactea simulation, we still find that some dwarfs are true pre-reionization fossils but the argument is weak if we use the Aquarius simulation results. In Table 2.1 we summarize the counts for dark matter and luminous satellites discussed in this section.

Although there is considerable uncertainty in our estimates, it can be safely concluded that, using the results of the Via Lactea simulation, at least a fraction of Milky Way dwarfs are fossils. However, this argument does not hold anymore or is weakened due to recent results (not yet published in a refereed journal) from the Aquarius simulations, showing a factor 2.5 increase for the number of Milky Way dark matter satellites in any mass range.

Table 1. Number of observed satellites versus number of dark halos with $v_c^{max}(t) > 20 \text{ km/s}$ (*i.e.*, non pre-reionization fossils) for the Milky Way

distance from Galactic center	number of luminous dwarfs		number of dark halos N_{dm} with $v_c^{max} > 20 \text{ km/s}$			
	this work	Tollerud et al.	Via Lactea sim.		Aquarius sim.	
			today	any time	today	any time
$d < 200 \text{ kpc}$	85 ± 14	120	14	36 ± 8	34	91 ± 20
$d < R_{vir} \sim 400 \text{ kpc}$...	from 300 to 600	28	73 ± 16	69	182 ± 40

2.2. Peculiar ultra-faint dwarfs

Almost all newly discovered dwarfs are dSphs with a dominant old population of stars and virtually no gas, which makes them viable candidates for being pre-reionization fossils. However, there are two notable exceptions that we discuss below.

2.2.1. *Leo T*

With the gas and young stars of a typical dIrr and the radius, magnitude, mass and metallicity of a dSph (Irwin et al. 2007; Simon & Geha 2007), *Leo T* presents a puzzle. *Leo T* has a stellar velocity dispersion of $\sigma_{LeoT} = 7.5 \pm 1.6 \text{ km s}^{-1}$ (Simon & Geha 2007), or an estimated dynamical mass of $10^7 M_{\odot}$ within the stellar spheroid (although its total halo mass may be much larger). *Leo T* shows no sign of recent tidal disruption by either the Milky Way or M31 (de Jong et al. 2008) and is located in the outskirts of the Milky Way at a Galactocentric distance of 400 kpc. *Leo T* photometric properties are identical to those of pre-reionization fossils. However, if we assume that *Leo T* is a pre-reionization fossil, it is not expected to retain significant gas or form stars after reionization.

How did *Leo T* keep its H I and how did its < 9 Gyr old stellar population form? Work by Stinson et al. (2007) suggests cyclic heating and re-cooling of gas in dwarf halos can produce episodic bursts of star formation separated by periods of inactivity. The lowest simulated dwarf to form stars has $\sigma = 7.4 \text{ km s}^{-1}$, similar to *Leo T*. However, the increasing of the IGM Jeans mass after reionization should prevent gas from condensing back into halos with circular velocity $v_c < 20 \text{ km s}^{-1}$. Another proposal (Ricotti 2008) is that, although the mass of *Leo T* at formation was $\sim 10^7 - 10^8 M_{\odot}$ (*i.e.*, a fossil), as indicated by its stellar velocity dispersion, its present dark matter mass and the halo concentration has increased after virialization by roughly a factor of $10/(1+z)$. This is expected if *Leo T* has evolved in isolation after virialization, as it seems to be indicated by its large distance from the Milky Way. In this scenario, *Leo T* stopped forming stars after reionization, but it was able to start accreting gas again from the IGM very recently (at $z \lesssim 1 - 2$). This can explain the < 9 Gyr old stellar population and the similarity of *Leo T* to the other pre-reionization fossils.

2.2.2. *Willman I*

Assuming virial equilibrium *Willman I* has a dynamical mass within the largest stellar orbit ($r \sim 100 \text{ pc}$) of $5 \times 10^5 M_{\odot}$ and a M/L of ~ 470 , similar to other ultra-faint dwarfs. However, *Willman I* has a distance from the Galactic center, luminosity, surface brightness and size typical of a galactic globular clusters (Willman et al. 2005a). The combination of dark matter domination with a small core radius, and a mass an order of magnitude smaller than the other SDSS dwarfs

suggests Willman I exists in the region between dwarf spheroidals and globular clusters. For our discussion of the missing galactic satellites, we treat Willman I as a dwarf because of its large dark matter fraction. However, its properties do not agree with being a “fossil” of the first galaxies (see Figure 1 in the next section).

3. Comparison with Theory

In this section, we compare the properties of the new dwarf galaxies discovered in the Local Group to the theoretical predictions of simulations of primordial galaxies formed before reionization. The argument that justifies this comparison is as follows.

After reionization, due to IGM reheating, the formation of galaxies smaller than 20 km s^{-1} is inhibited because the thermal pressure of the IGM becomes larger than the halo gravitational potentials (*e.g.*, Gnedin 2000). Galaxies formed before reionization stop forming stars due to the progressive photo-evaporation of their interstellar medium by the ionizing radiation background (although most of the ISM was already lost due to UV driven galactic winds and SN explosions). Hence, if pre-reionization dwarfs do not grow above $v_c = 20 \text{ km s}^{-1}$ by mergers, their stellar population evolves passively as calculated by stellar evolution models such as Starburst99 (Leitherer et al. 1999). We define such galaxies as pre-reionization “fossils”.

Clearly, we do not expect two perfectly distinct populations of fossils with $v_c < 20 \text{ km s}^{-1}$ and non-fossils with $v_c \geq 20 \text{ km s}^{-1}$, but a gradual transition of properties from one population to the other. Some fossils may become more massive than $v_c \sim 20 \text{ km s}^{-1}$ after reionization, accrete gas from the IGM, and form a younger stellar population. If the dark halo circular velocity remains close to 20 km s^{-1} the young stellar population is likely to be small with respect to the old one. We call these galaxies “polluted fossils” because they have the same basic properties of “fossils” with a sub-dominant young stellar population (see RG05).

Vice versa, some non-fossil galaxies with $v_c > 20 \text{ km s}^{-1}$ may lose a substantial fraction of their mass due to tidal interactions. If they survive the interaction, their properties, such as surface brightness and half light radius, may be either modified or stay the same. Kravtsov et al. (2004) estimate that 10% of Milky Way dark matter satellites were at least ten times more massive at their formation than they are today and more were a few times more massive than they are today. Although their simulation does not include stars, they favor the idea that the stellar properties of these halos would be unchanged. Conversely, a recent work of Peñarrubia et al. (2008) looks at tidal stripping of dark matter and stars, achieving some success in reproducing the observed properties of ultra-faint dwarfs assuming that they are tidally stripped dIrrs. Using our simulations, we cannot make predictions of the internal properties of non-fossil dwarfs, which are too massive to be present in significant numbers in the small volume of our simulation. However, using our simulation data (in RG05), GK06 finds that about one third of Milky Way satellites may be fossils based on comparisons between observed and simulated Galactocentric distribution of the satellites.

3.1. Description of the simulation

Given a cosmological model, simulating the formation of the first stars is a relatively well defined initial condition problem. However, these simple initial conditions become unrealistic as soon as a few stars form within a volume of several thousands of co-moving Mpc^3 . The physics becomes complex as competing feedback effects determine the fate of the first galaxies: radiative feedback regulates the formation and destruction of H_2 in the intergalactic medium and in proto-galaxies. The background in the Lyman-Werner bands (between 11.3 eV and 13.6 eV) dissociates H_2 through the two-step Solomon process. A few Population III stars per Mpc^3 can suppress or delay the formation of the first small mass galaxies, reducing drastically their number per unit co-moving volume (Haiman et al. 2000; Ciardi et al. 2000; Machacek et al. 2000).

Ionizing radiation may enhance the production of H_2 (we refer to this as “positive feedback”) by creating free electrons and promoting the formation of H^- , the main catalyst for the formation of H_2 (Shapiro & Kang 1987; Haiman, Rees, & Loeb 1996; Ricotti, Gnedin, & Shull 2001; Alvarez, Bromm, & Shapiro 2006; Ciardi et al. 2006). Ricotti et al. (2001) studied the structure of H II regions in the early universe in a gas of primordial composition. It was found that shells of H_2 can be continuously created in precursors around the Strömgren spheres produced by ionizing sources and, for a bursting mode of star formation, inside recombining H II regions. This is because the catalyst H^- , and hence H_2 , is formed in regions where the gas ionization fraction is about 50%. The thickness of these regions depends on the density of the gas and the spectrum of the ionizing radiation. This local “positive feedback” may be the dominant feedback, but it is difficult to incorporate into cosmological simulations because the implementation of spatially inhomogeneous, time-dependent radiative transfer is computationally expensive.

The simulation analyzed in the present paper differs from other studies because it includes “positive feedback” from ionizing radiation self-consistently (Ricotti et al. 2002a,b, 2008)(hereafter, RGS02a,b, RGS08). The simulation have a space resolution of 156 pc h^{-1} comoving (about 15 pc physical at $z = 10$) and a mass resolution of $4.93 \times 10^3 \text{ M}_\odot \text{ h}^{-1}$ for dark matter and $\approx 657 \text{ M}_\odot \text{ h}^{-1}$ for the baryons. There are more than 10^5 stellar particles in our simulations at $z \sim 10$. The stellar masses are always smaller than the baryon mass resolution but can vary from $\sim 0.6 \text{ M}_\odot \text{ h}^{-1}$ to $600 \text{ M}_\odot \text{ h}^{-1}$ with a mean of $6 \text{ M}_\odot \text{ h}^{-1}$. Stellar particles do not represent real stars. In addition to primordial chemistry and 3D radiative transfer, the simulations include a recipe for star formation, metal production by SNe and metal cooling (see RGS02a for details). The code also includes mechanical feedback by SN explosions. However, we found that for a Salpeter IMF, the effect of SNe is not dominant when compared to feedback produced by ionizing radiation from massive stars (Ricotti et al. 2008). The effect of SN explosion is somewhat model dependent and uncertain because it is treated using a sub-grid recipe. Hence, the simulation analyzed in this work includes metal pollution but not mechanical feedback by SNe.

RGS02b have shown that the main negative feedback thought to suppress the formation of the first galaxies (H_2 photo-dissociation) is not dominant, contrary to the results of previous studies

that did not include “positive feedback” from ionizing radiation. Feedback by ionizing radiation plays the key role, inducing a bursting star formation mode in the first dwarf galaxies. Galactic outflows, produced by UV photo-heating from massive stars, and H₂ formation/photo-dissociation induce the bursting star formation mode that acts as the catalyst for H₂ re-formation inside relic (recombining) H II regions and in the “precursors” of cosmological Strömgren spheres (*i.e.*, positive feedback regions). As a result, star formation in the first galaxies is self-regulated on a cosmological scale - it is significantly reduced by feedback but it is not completely suppressed, even in small mass halos with $v_c \sim 5 - 10 \text{ km s}^{-1}$. Due to the feedback-induced bursting mode of star formation in pre-reionization dwarfs, the cosmological H II regions that they produce remain confined in size and never reach the overlap phase that defines the epoch of reionization.

The simulation data shown in this paper is the higher resolution run in RGS02b, evolved further to redshift $z = 8.0$ after the introduction of a bright source of ionizing radiation that completes reionization at $z \sim 9$ (see RG05 for details). The need for introducing a bright ionization source is dictated by the small volume of the simulation (1.5^3 Mpc^3); otherwise the volume would be reionized too late. The H I ionizing source removes all the remaining gas from halos with $v_c < 20 \text{ km s}^{-1}$ and shuts down star formation.

3.2. Statistical properties of simulated “fossils” vs observations

Here we compare the RG05 predictions for the fossils of primordial galaxies to the observed properties (see Table 4) of the new Milky Way and M31 dwarfs. The symbols and lines in Figs. 1-6 have the following meanings. All known Milky Way dSphs are shown by circles; Andromeda’s dSphs satellites are shown by triangles; simulated fossils are shown by the small solid squares. The solid and open symbols refer to previously known and new dSphs, respectively. The transition between fossils and non-fossil galaxies is gradual. In order to illustrate the different statistical trends of “non-fossil” galaxies we show dwarf irregulars (dIrrs) with asterisks and the dwarf ellipticals (dE) as crosses, and we show the statistical trends for more luminous galaxies as thick dashed lines on the right side of each panel.

Figure 1 shows how the surface brightness (top panel) and half light radius (bottom panel) of all known Milky Way and Andromeda satellites as a function of V-band luminosity compares to the simulated fossils. The surface brightness limit of the SDSS is shown by the thin solid lines in both panels of the figure. The new dwarfs agree with the predictions up to this threshold, suggesting the possible existence of an undetected population of dwarfs with Σ_V below the SDSS sensitivity limit. The new M31 satellites have properties similar to their previously known Milky Way counterparts (*e.g.*, Ursa Minor and Draco). Given the similar host masses and environments, is reasonable to assume a similar formation history for the halos of M31 and the Milky Way. This suggests the existence of an undiscovered population dwarfs orbiting M31 equivalent to the new SDSS dwarfs.

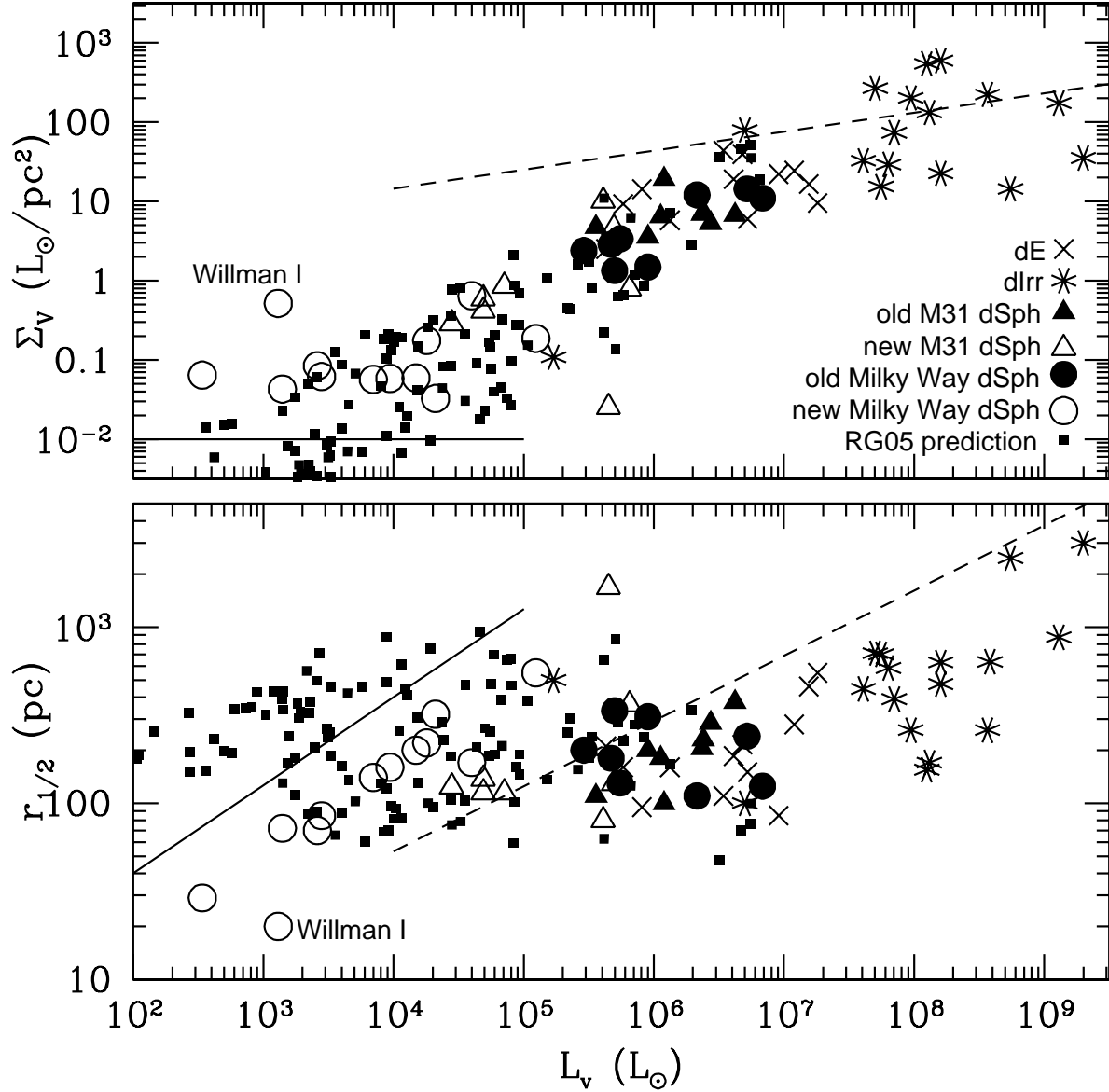


Fig. 1.— An extension of Figure 7 from RG05 to include new dwarfs in the SDSS (Belokurov et al. 2007, 2006; Irwin et al. 2007; Willman et al. 2005b,a; Walsh et al. 2007; Zucker et al. 2006b,a; Geha et al. 2009) and recent surveys of Andromeda (Ibata et al. 2007; Majewski et al. 2007; Martin et al. 2006). Surface brightness and core radius are plotted vs. V-band luminosities. Small filled squares are the RG05 predictions, asterisks are known survivors, crosses are known polluted fossils, closed circles are the previously known dSph around the Milky Way, closed triangles are previously known dSph around M31, and open circles and triangles are new dSph around the Milky Way and M31 respectively. The solid lines show the SLOAN surface brightness limits and the dashed lines show the scaling relationships for more luminous Sc-Im galaxies ($10^8 L_\odot \lesssim L_B \lesssim 10^{11} L_\odot$) derived by Kormendy & Freeman (2004).

3.2.1. Extreme Mass-to-Light ratios

The large mass outflows due to photo-heating by massive stars and the consequent suppression of star formation after an initial burst, make reionization fossils among the most dark matter dominated objects in the universe, with predicted M/L ratios as high as 10^4 and $L_V \sim 10^3 - 10^4 L_\odot$.

Figure 2 shows the velocity dispersion (bottom panel) and mass-to-light ratios, M/L_V (top panel), as a function of V-band luminosity of the new and old dwarfs from observations in comparison to simulated fossils. The symbols are the same as in the previous figures. While mass data is available for all the previously known dwarfs, we found no published σ values for 9 dIrr, 4 dE and 3 dSph (Antila, Phoenix and SagDIG) (Mateo 1998; Strigari et al. 2008). We observe a good agreement between the statistical properties of the new dwarf galaxies and the RG05 predictions for the fossils, although simulated dwarfs show a slightly larger mass-to-light ratios than observed ones at the low luminosity end, $L_V < 10^4 L_\odot$. Theoretical and observed dynamical masses are calculated the same way, from the velocity dispersions of stars (*i.e.*, $M = 2r_{1/2}\sigma^2/G$), and do not necessarily reflect the total mass of the dark halo at virialization. Indeed, the simulation provides some insight on why the observed value of the dynamical mass, $M \sim (1 \pm 5) \times 10^7 M_\odot$, remains relative constant as a function of L_V . Simulations show that in pre-reionization dwarfs, the ratio of the radius of the stellar spheroid to the virial radius of the dark halo decreases with increasing dark halo mass. The lowest mass dwarfs have stellar spheroids comparable in size to their virial radii (see RGS08). As the halo mass and virial radius increases, the stellar spheroid becomes increasingly concentrated in the deepest part of the potential well, thus the ratio of the dynamical mass within the largest stellar orbits to total dark matter mass is reduced. This effect maintains the value of the dynamical mass within the stellar spheroid (measured by the velocity dispersion of the stars) remarkably constant even though the total mass of the halo increases.

If dwarfs are undergoing tidal disruption (*e.g.*, Ursa Major II), the velocity dispersions could be artificially inflated. However, the agreement with theory is rather good for all the new ultra-faint dwarfs. The data on the lowest luminosity dwarfs in our simulations are the least reliable, because they are very close to the resolution limits of the simulation (we resolve halos of about $10^5 M_\odot$ with 100 particles). Let us assume we can trust the simulation and the observational data, even for the lowest luminosity dwarfs and the discrepancy between simulation and observation at the low luminosity end is real. The dynamical mass is $M \propto r_{1/2}\sigma^2$. There is good agreement between observations and simulations for σ in faint dwarfs. Thus, it is likely that the the reason for disagreement in M/L_V is due to the value of $r_{1/2}$, being smaller for the observed dwarfs than the simulated ones. This could be partly due an observational bias that selects preferentially dSphs with higher surface brightness and smaller $r_{1/2}$ (see Figure 1). Another explanation, is a dynamical effect not included in our simulation that reduces the stellar radius of dwarfs after virialization; for instance, tidal stripping or relaxation. A larger sample size of distant dwarfs, including kinematics on And XII and And XIV, both believed to be on their first approach to M31, would be useful to better characterize this discrepancy.

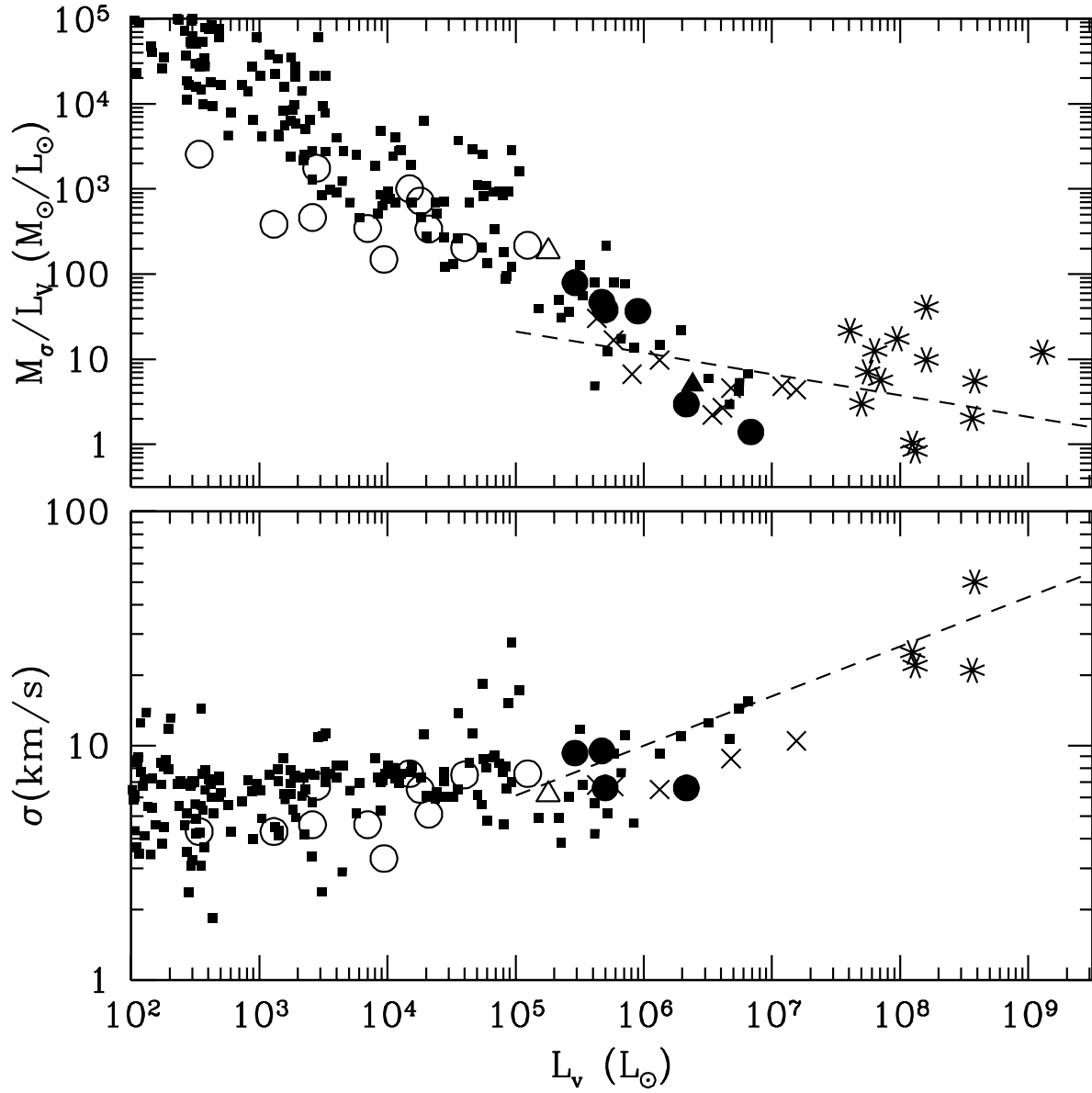


Fig. 2.— Mass-to-light ratio and velocity dispersion of a subset of the new dwarfs (Martin et al. 2007; Simon & Geha 2007) plotted with values for previously known dwarfs and RG05 predictions. The dashed lines show the scaling relationships for more luminous Sc-Im galaxies ($10^8 L_\odot \lesssim L_B \lesssim 10^{11} L_\odot$) derived by Kormendy & Freeman (2004).

The velocity dispersions of the stars for the observed new dwarfs and the simulated fossils are just below 10 km s^{-1} for luminosities $< 10^6 L_V$. The scatter of the predicted and observed velocity dispersions as a function of dwarf luminosity suggests that dwarfs with the same luminosity may be found in a broad distribution of halos masses. These results are in agreement with Figure 4, showing that the faintest primordial galaxies of a given luminosity may form in halos with a total mass at virialization between $10^6 - 10^7 M_\odot$ to a few times $10^8 M_\odot$. This is because at these small masses the star formation efficiency is not necessarily proportional to the dark halo mass and there is a large scatter in f_* at any given mass. This is due to the nature of feedback effects that is local and depends on the environment (*e.g.*, positive feedback on the formation of H_2). In RG08 is found that pre-reionization dwarfs that form in relative isolation have typically smaller value of f_* than dwarfs of the same total mass that form in the vicinity of other luminous dwarfs (see Fig. 4 in RGS08).

3.2.2. Understanding the luminosity-metallicity relation

The metallicity-luminosity relation of the observed and simulated dwarfs is shown in Figure 3. $[\text{Fe}/\text{H}]$ is plotted against V-band luminosity in solar units. Symbols for the previously known dwarfs, the new, ultra-faint dwarfs, and simulated fossils are the same as in Figure 1. In this plot, we also color code simulated fossils according to their star formation efficiency, f_* , defined as $f_* = M_*/M_{bar}$, where M_* is the mass in stars and $M_{bar} \approx M_{dm}/6$ is the baryonic mass of the halo assuming cosmic baryons abundance. Red symbols show simulated dwarfs with $f_* < 0.003$, blue $0.003 \leq f_* \leq 0.03$ and green $f_* > 0.03$.

The new ultra-faint dwarfs do not follow a tight luminosity-metallicity relationship observed in more luminous galaxies (but see Geha et al. (2009)). This behavior is in good agreement with the predictions of our simulation. The recently found dwarf galaxy Segue 1 with luminosity of $340L_\odot$ and metallicity of $[\text{Fe}/\text{H}] \sim -2.8$ fills a gap in the luminosity-metallicity plot that was previously devoid of observed dwarfs, present instead in the simulation (Geha et al. 2009). However, Segue 1 has a half light radius that is smaller than what our simulation predicts. Compared to their previously known counterparts, the new dwarfs have a slightly lower metallicity but much lower luminosities.

There are several physical mechanisms that may produce the observed scatter in metallicities of dwarfs at a given constant luminosity. Here, we identify the two mechanism that are dominant in our simulation for primordial dwarf galaxies: 1) the large spread of star formation efficiencies producing a dwarf of a given luminosity is the dominant mechanism (to zero-th order approximation, in a closed box model, we have $Z \propto f_*$) and 2) the existence of dwarfs experiencing either a single or multiple episodes of star formation contribute to the metallicity spread as well. Metal pollution from nearby galaxies at formation might also play a role. For more massive dwarfs that form after reionization, there may be different processes that dominate metal enrichment. See Tassis et al. (2008) for a discussion.

Let’s start from the first mechanism. Contrary to what it is usually the case for more massive galaxies, we find that in primordial dwarfs with masses $\lesssim 5 \times 10^7 M_\odot$ the star formation efficiency f_* does not monotonically increase with halo mass (*i.e.*, f_* has a large spread for a given halo mass or for a given mass in stars, M_* , see RGS08 Figure 4 and Figure 7). The wide range in values results from the sensitivity of f_* on a halo’s environment and is due to local feedback effects that are of fundamental importance in determining star formation in shallow potential wells typical of pre-reionization dwarfs. Figure 4 (taken from Figure 7 in RGS08) shows that below a few $10^7 M_\odot$, halos with exactly the same dark mass can be either dark or luminous (depending on the environment). Thus, feedback from non-ionizing and ionizing UV radiation, mechanical feedback and chemical enrichment can produce two halos with the same dark mass and very different star formation efficiencies. This appears to be the main effect responsible for the observed spread in metallicity for a given luminosity, in the new dwarfs. In Figure 5, we plot the metallicity as a function of the mean star formation efficiency for the halo, f_* . As expected, simulated dwarfs with higher values of the star metallicity are the ones with the larger value of f_* .

However, this effect alone cannot account for all the observed scatter of the metallicity as illustrated by the color coding of simulated dwarfs in Figure 3. It appears that the metallicity is not simply proportional to f_* (otherwise the boundaries between symbols of different color would be horizontal). Instead, for a given value of f_* , the metallicity is larger for fainter dwarfs. It is not too surprising that Z is not simply proportional to f_* . Even when using a very simple chemical evolution model, neglecting gas inflows and assuming instantaneous metal recycling, the mean metallicity of the stars is proportional to M_*/M_{gas} rather than $f_* = M_*/M_{bar}$, where M_{gas} is the initial value of the gas mass available for star formation. Thus, $Z \propto f_*(M_{bar}/M_{gas})$. If feedback effects reduce the value of M_{gas}/M_{bar} below unity in the smallest and lowest luminosity primordial dwarfs, the metallicity of the stars will be larger for a fixed value of f_* , as observed in Figure 5 and Figure 3. The reduction of M_{gas}/M_{bar} below unity can be produced by three effects: the increase of the Jeans mass of the IGM over the virial mass of the halo due to reheating (see Figure 6 in RGS08), heating of the gas via ionizing radiation from stars within the halo, and by multiple episodes of star formation with a first burst that lowers M_{gas} substantially, but does not produce sufficiently large values of f_* and Z when compared to subsequent bursts.

Figure 6 shows $[\text{Fe}/\text{H}]$ versus the surface brightness in the V-band, Σ_V . The symbols are the same as in Fig. 1 and the solid line shows the SDSS sensitivity limit. No trend is observed between metallicity and Σ_V for the simulated dwarfs. Observed dwarfs show less scatter for Σ_V -metallicity relation than for the luminosity-metallicity relation in Figure 3. There is one dwarf with metallicity below $[\text{Fe}/\text{H}] = -2.5$: Segue-1 that has $[\text{Fe}/\text{H}] = -2.8$. Since the spectral synthesis method used in Kirby et al. (2008) and Geha et al. (2009) may not be subject to the overestimation of metallicities seen with measurements using the CA triplet, the lack of dwarfs with $[\text{Fe}/\text{H}] < -3.0$ could be a sign of a change in the IMF at very low $[\text{Fe}/\text{H}]$.

Finally, we have examined whether there is a dependence of the metallicities on the distance of the galaxy from the Milky Way or Andromeda. For the new Milky Way dwarfs there is slight trend

of higher metallicities at smaller Galactocentric distances; however, the upward trend is dominated by Ursa Major II and Coma Ber., both of which show evidence for tidal disruption. For the M31 dwarfs, no trend was observed.

Figures 7 show the scatter of the metallicity of the stars, $\sigma_{[Fe/H]}$, plotted against V-band luminosity and $[Fe/H]$ respectively. Once more, the various point types and colors are the same used in Figure 3. The observational data for the new dwarfs matches the predictions, though Figure 7 shows a lack of low L_V objects with $\sigma_{[Fe/H]} < 0.4$. However, given the small number of data points available, it is not possible to rule out selection effects of small number statistics as an explanation. Dwarfs with low values of $\sigma_{[Fe/H]}$ tend to have higher luminosities and are equally likely to be a dE or dSphs. However, dwarfs with the highest $\sigma_{[Fe/H]}$ are faint dSphs with $L_V < 10^6 L_\odot$, and occupy the lowest mass dark matter halos. It is not clear at this point how reliable the simulation data for $\sigma_{[Fe/H]}$ is for dwarfs with luminosities $L_V < 10^3 - 10^4 L_\odot$. However, all the dwarfs we analyze have at least 10 stellar particles and 100 dark matter particles. The masses of stellar particles vary, depending on the star formation efficiency and the duration of the star burst.

As with the metallicities, we looked at how the metallicity spread depends on the distance from the host. For both previously known and ultra-faint dSphs there is no dependence on distance within the virial radius of the Milky Way. There is a lack of dwarfs with high $\sigma_{[Fe/H]}$ beyond 400 kpc; however, given the small number of data points and the luminosity and surface brightness limits of current surveys, the trend is not statistically significant.

3.3. The Missing Galactic Satellite Problem Revisited

In order to simulate a representative sample of the universe, the size of cosmological simulations must be significantly larger than the largest scale that becomes non-linear at the redshift of interest. At $z = 0$, this scale is at least 50 to 100 Mpc. Current computational resources are not able to evolve a cosmological simulation of this size that includes all the relevant gas and radiation physics, to $z = 0$. However, as argued in § 3, the properties of those fossil galaxies that survive tidal destruction change only through passive aging of their stars formed before reionization (but see Ricotti 2008), allowing their properties at $z = 0$ to be simply related to their properties at reionization. GK06 uses this approximation in conjunction with high-resolution N-body simulations of the Local Group, to evolve a population of dwarf galaxies around a Milky Way mass halo from $z = 70$ to $z = 0$. For details of the simulations, see § 2 in GK06.

GK06 define a fossil as a simulated halo which survives to $z = 0$ and remains below the critical circular velocity of 20 km s^{-1} with no appreciable tidal stripping. They calculate the probability, $P_S(v_{c,max}, r)$, of a luminous halo with a given maximum circular velocity $v_{c,max}$ to survive from $z = 8$ (the final redshift of the RG05 simulation) to $z = 0$. For a given $v_{c,max}$, the number of dwarfs at $z = 0$ is $N(v_{c,max}, z = 8)P_S(v_{c,max}, r)$. The surviving halos are assigned a luminosity based on the

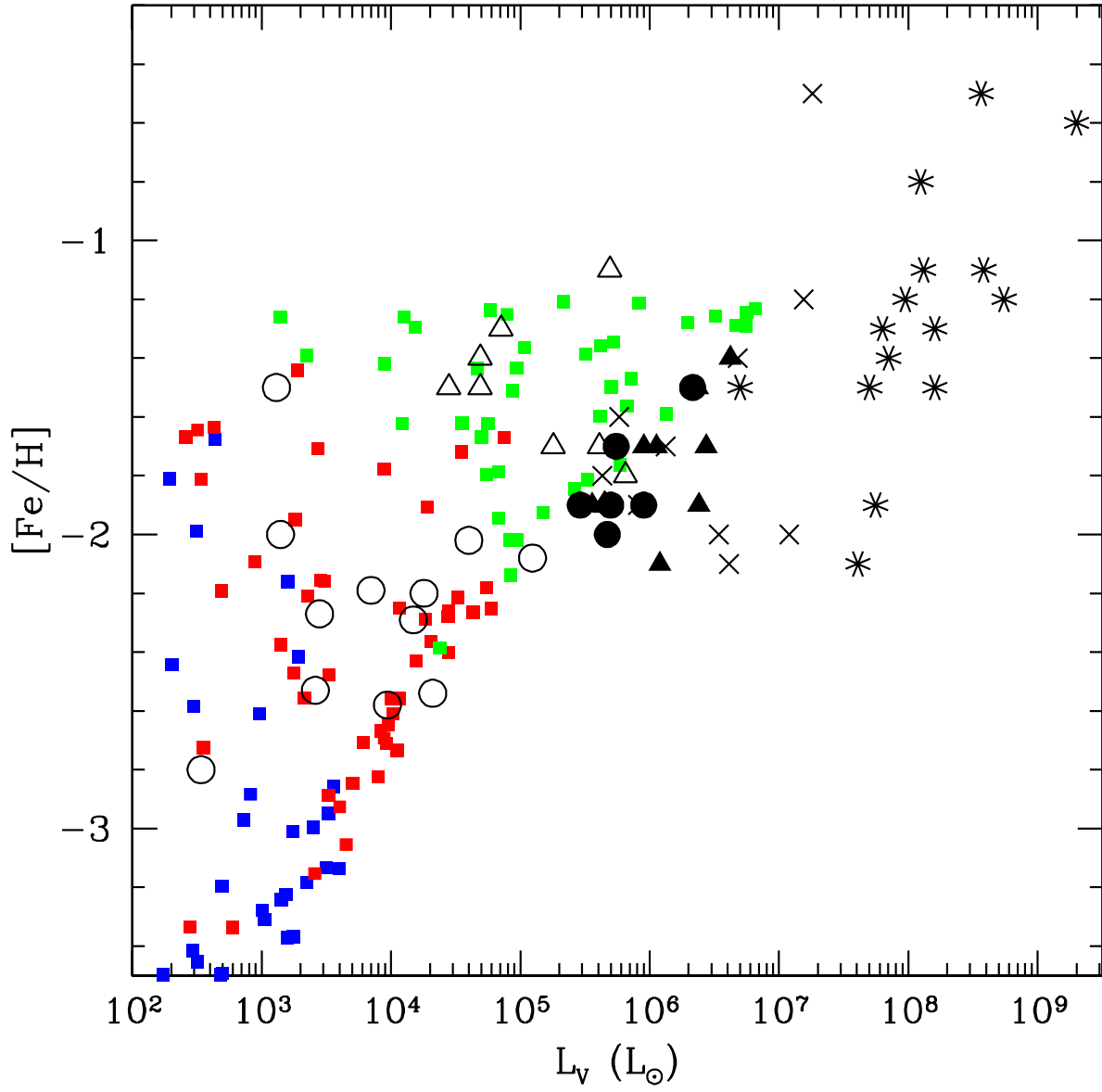


Fig. 3.— Metallicity vs. luminosity for the new and old dwarfs plotted against RG05 predictions.

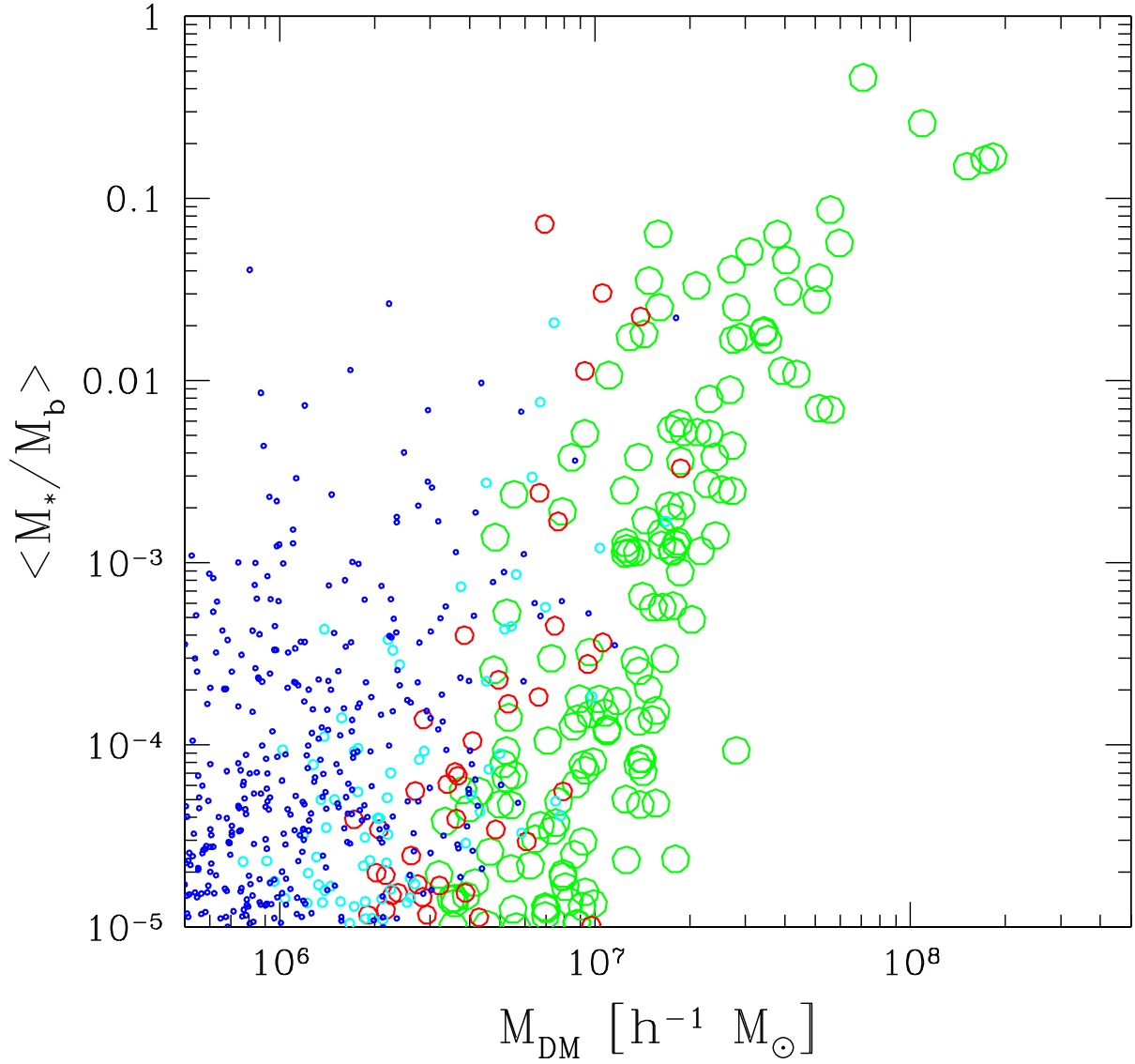


Fig. 4.— Fraction of baryons converted into stars as function of halo mass of the galaxy at $z = 10$. Circles, from smaller to the larger, refer to galaxies with gas fractions $f_g = M_{\text{gas}}/M_b < 0.1\%$ (blue), $0.1\% < f_g < 1\%$ (cyan), $1\% < f_g < 10\%$ (red) and $f_g > 10\%$ (green), respectively.

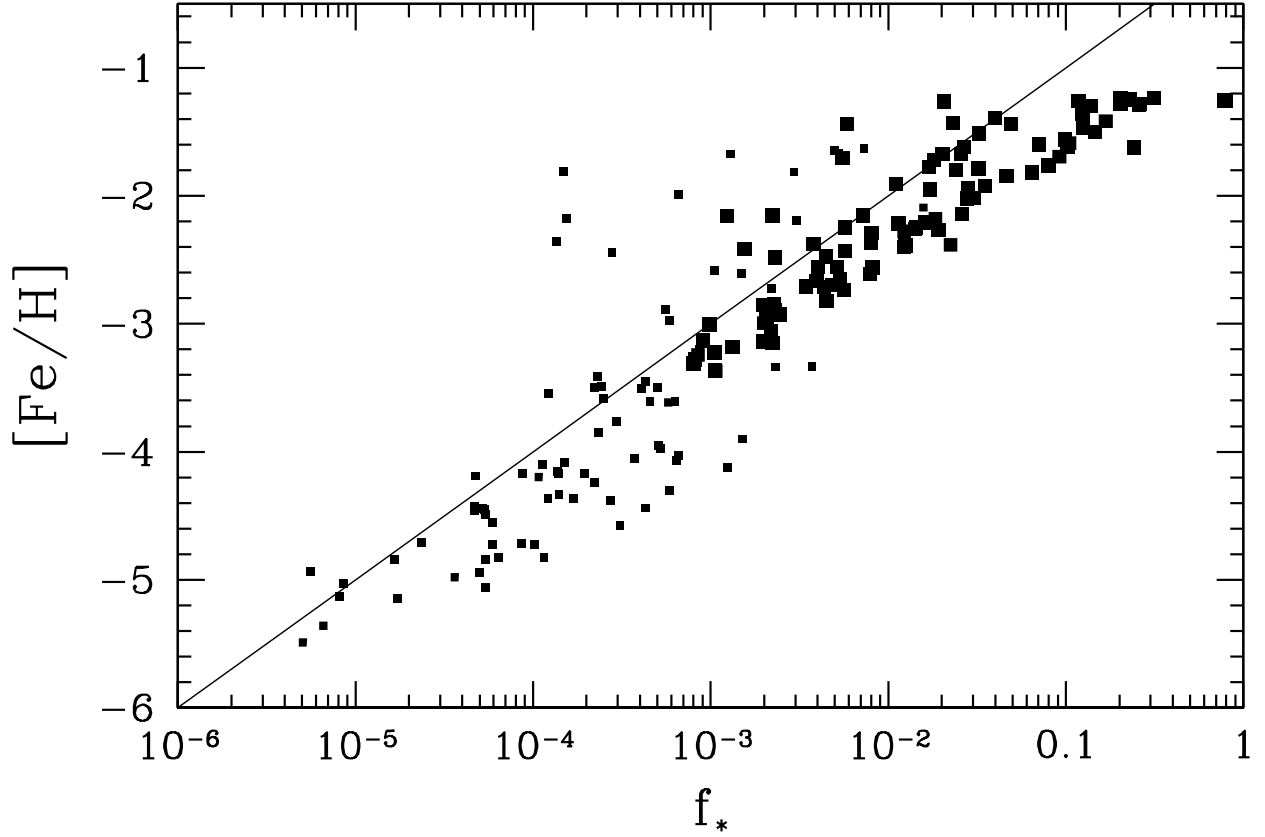


Fig. 5.— Metallicity versus star formation efficiency $f_* = M_*/M_b$ for the simulated fossils. The large squares show galaxies with $L_V \geq 10^3 L_\odot$, and the small squares galaxies with $L_V < 10^3 L_\odot$.

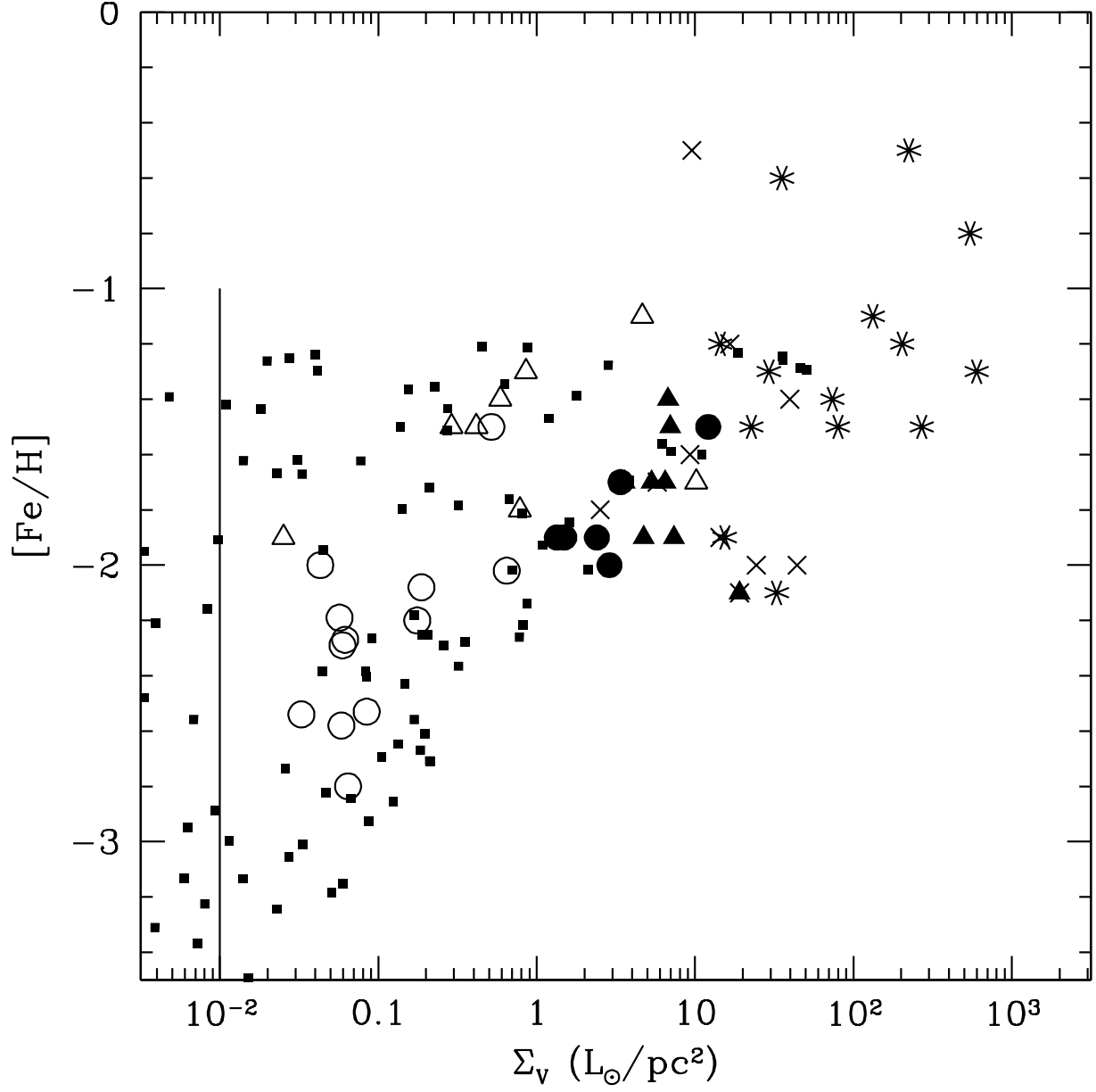


Fig. 6.— Metallicity vs. surface brightness for the new and old dwarfs. The surface brightness limit of the SDSS is shown by a solid vertical line. Note the predicted dwarfs with $Z < -2.5$ and surface brightnesses above Sloan detection limits.

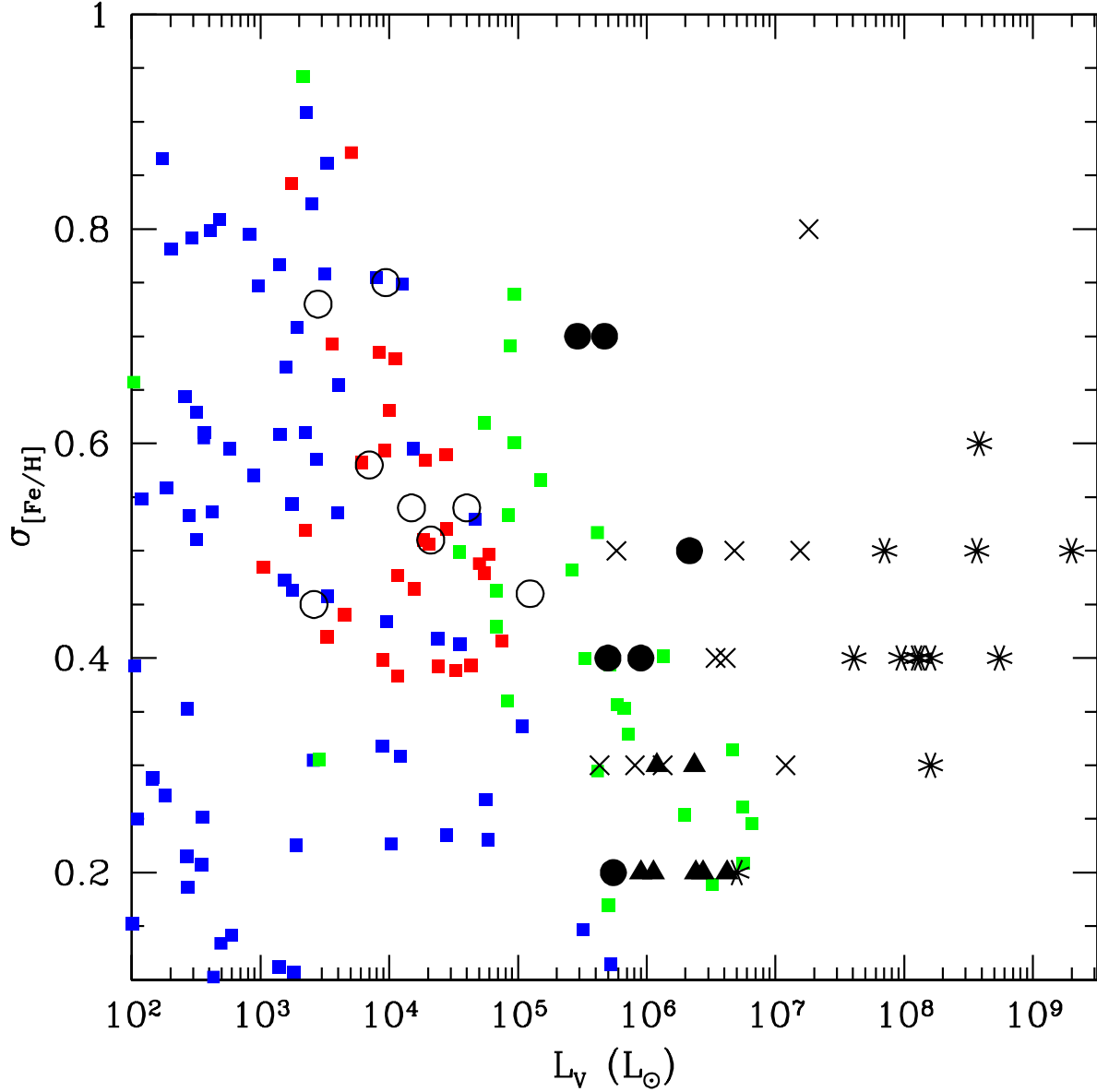


Fig. 7.— Metallicity spread vs. V-band luminosity for the new and old dwarfs. Simulation data for the metallicity spread may be unreliable for dwarfs with luminosities $L_V < 10^3 - 10^4 L_\odot$, due to the small number of stellar particles in the galaxies.

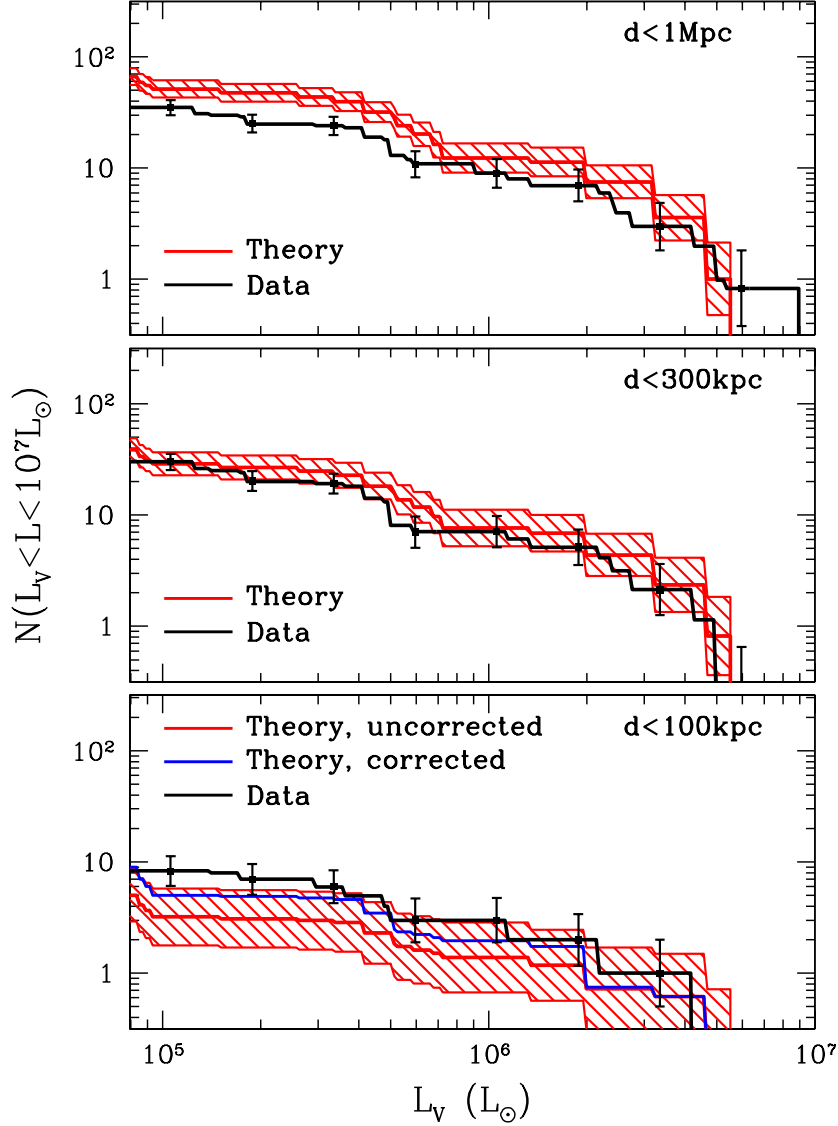


Fig. 8.— Luminosity function of pre-reionization fossil dwarfs predicted in GK06 (red) plotted with the luminosity function for the new and old Local Group dSphs. The black lines are the observations corrected for completeness as discussed in Section 2. Corrections to the theory account for an under-abundance of small halos near the hosts due to numerical effects (GK06).

L_V versus $v_{c,max}$ relationship from RG05. At $z = 0$, GK06 has a population of dwarf galaxies with a resolution limit of $v_{c,max} = 13 \text{ km s}^{-1}$. Unfortunately, this limit corresponds to a lower luminosity limit of $L_V \sim 10^5 L_\odot$, which includes Leo T and Canes Venatici I, but excludes all the other new ultra-faint Milky Way satellites. We do not show the prediction of the GK06 model below this lower luminosity limit. A new N-body method with a resolution limit of $L_V \sim 10^3 L_\odot$ that follows the merger histories for the halos will be presented in Bovill & Ricotti (2008), in preparation.

In Figure 8, we show the cumulative luminosity function from GK06 for the Milky Way and M31 satellites with the addition of the new ultra-faint dSphs. The lower panel shows satellites with distance from their host $d < 100 \text{ kpc}$, the middle panel $d < 300 \text{ kpc}$ and the upper panel $d < 1 \text{ Mpc}$. The gray lines show the GK06 predictions, and the shaded region encompasses the error bars. Since, the resolution limits of GK06 causes halos with $v_{c,max} < 17 \text{ km s}^{-1}$ to be preferentially destroyed by tidal effects, the predicted luminosity function is corrected. Both the uncorrected (lower) and corrected (upper) luminosity functions are plotted in the lower panel. On all three panels, the black histogram and the points with error bars represent the observed luminosity function of fossil dwarfs around the Milky Way and M31. Their numbers have been corrected for completeness as discussed in § 2. For the purposes of this plot, we are considering all the new dwarfs to be fossil candidates.

For $d < 100 \text{ kpc}$ (bottom panel), there is an overabundance of observed satellites with respect to the simulated luminosity function from 10^5 to $10^6 L_\odot$. This discrepancy is likely due to excessive destruction rate of satellites caused by the insufficient resolution the GK06 N-body simulations. At distances $d < 300 \text{ kpc}$ (middle panel), there is excellent agreement between theory and observation. Canes Venatici I and the new Andromeda satellites are included in the latter panel. The upper panel shows the luminosity function for all dwarfs within 1 Mpc of the host, including Leo T. Note, that GK06 assumes an isolated Milky Way type galaxy (with total mass comparable to the Local Group mass), while observations with $d < 1 \text{ Mpc}$ of the Milky Way include the satellite system around M31. For $d < 1 \text{ Mpc}$, there is an under-abundance of observed satellites between 10^5 to $10^6 L_\odot$ with respect to the simulation predictions. However, this is consistent with the theory since beyond 250 kpc dwarfs with $L_V \sim 10^5 L_\odot$ drop below SDSS detection limits (Koposov et al, 2007). Hence, the under-abundance of observed dwarfs at large distances may be due to the completeness limit of the survey.

4. Discussion and Conclusions

There are two main ideas for the origin of dSphs in the Local Group. Most importantly, these two ideas have very different implications for models of galaxy formation, and the minimum mass a dark halo needs to host a luminous galaxy. The “tidal scenario”, holds the dwarfs we see today were once far more massive, having been stripped of most of their dark matter during interactions with larger galaxies (*e.g.*, Kravtsov et al. 2004). In this model, we would expect the halos with original dark matter masses below $10^8 M_\odot$ to be mostly dark at formation and at the modern epoch. The “primordial scenario”, has dwarf galaxies starting with close to their current stellar mass of

about $10^3 - 10^6 M_\odot$ and, with several dark halos with mass at formation below the threshold of about $2 \times 10^8 M_\odot$ hosting a luminous galaxy. Star formation in halos this small is possible only before reionization and is widespread if “positive” feedback plays a significant role in regulating star formation in the first galaxies (Ricotti et al. 2001, 2002a,b).

In this paper, we argue that the recent discovery of the ultra-faint dwarfs in the Milky Way and M31 supports the “primordial scenario”. The existence of the ultra-faint dwarfs was predicted by simulations of the formation of the first galaxies (see RG05) and, as shown in the present work, the observed properties of this new population are consistent with them being the “fossils” of the first galaxies.

While tidal stripping can reproduce properties of an individual galaxy, it is unable to completely reproduce all the trends in the ultra-faint population. This is primarily seen in the kinematics of the ultra-faint dwarfs. Tidal stripping predicts a steeper than observed drop in σ with L_V (Peñarrubia et al. 2008), while our simulations show primordial dwarfs which match the observed trends in σ extremely well. It has not been shown yet that star formation in dwarf galaxies more massive than $10^8 - 10^9 M_\odot$ can reproduce the observed properties of ultra-faint dwarfs without requiring tidal stripping of stars.

The tidal model predicts that gas rich dIrr loose their gas and transform into dSphs due to tidal or ram pressure interaction with a host halo. And XII, which shows a proper motion close to current published escape velocity of M31, may be on its first approach to the Local Group (Martin et al. 2006; Chapman et al. 2007). A similar situation exists for And XIV. With a dynamical mass of $M \sim 3 \times 10^7 M_\odot$, And XIV has $v > v_{esc}^{M31}$, suggesting it is also just entering the Local Group (Chapman et al. 2007). In the tidal model (Mayer et al. 2007, 2006), And XII and And XIV would be expected to still harbor significant reservoirs of gas, however, observations show And XIV has $M_{HI} < 3 \times 10^3 M_\odot$ (Chapman et al. 2007) and And XII has no detected H I (Martin et al. 2006). If neither of these dwarfs have undergone significant tidal interactions with their hosts, as their velocities suggest, how did they lose their gas? Though its velocity is unknown, the recently discovered And XVIII (McConnachie et al. 2008), shows the same characteristics. At a distance of 600 kpc from M31 and 1.35 Mpc from the Milky Way, it is unlikely that And XVIII has undergone significant interaction with either Local Group spirals. And XVIII is classified as a dSph with no detected H I and is similar to the Cetus and Tucana dwarfs (McConnachie et al. 2008), both of which are good candidate fossil galaxies (RG05).

On the opposite end of the spectrum is the strange case of Leo T, the properties of which are discussed in Section 2.1.1. While, Leo T has an H I mass fraction typical of dIrr, its other properties are indistinguishable from the other newly discovered ultra-faint dwarfs (Simon & Geha 2007), all of which are dSph. Leo T’s large distance from its host, H I reservoir and low probability of recent tidal interactions (de Jong et al. 2008) make it a good candidate for a precursor to a dSph in the tidal scenario. Particularly given that Leo T’s dynamical mass within the stellar spheroid is small: $8.2 \times 10^6 M_\odot$ (Simon & Geha 2007), its gas is unlikely to survive a single tidal encounter intact.

Therefore, Leo T may have formed at or near its current mass, and the striking similarity of Leo T to its ultra-faint counterparts suggests that they too could have formed as primordial dwarfs at their current masses.

By our definition, pre-reionization fossils are dwarfs that form before reionization in dark halos with $v_c < v_c^{cr} \sim 20 \text{ km s}^{-1}$, while non-fossils dwarfs form in halos with $v_c > v_c^{cr}$ before and after reionization. The value $v_c^{cr} \sim 20 \text{ km s}^{-1}$ that we use to define a fossil is primarily motivated by fundamental differences in cooling and feedback processes that regulate star formation in these halos in the early Universe. This value of the circular velocity is also very close to estimates based on the suppression of star formation in dwarfs after reionization (Gnedin 2000; Okamoto et al. 2008). However, as argued in (Ricotti 2009), fossils dwarfs can have a late phase of gas accretion and star formation well after reionization, at redshift $z < 1 - 2$. Thus, a complete suppression of star formation after reionization is not necessarily what defines a “fossil galaxy”.

The number of Milky Way dark satellites that have or had in the past $v_c > v_c^{cr}$ can be estimated using the results of published N-body simulations (see § 2.1). We find that using the Via Lactea N-body simulation there are approximately $N_{dark} \approx 73 \pm 16$ halos with $v_c > 20 \text{ km s}^{-1}$ within the virial radius (Diemand et al. 2007). The new Aquarius simulations (Springel et al. 2008), however, show a factor of 2.5 increase in the number of halos with $v_c > 20 \text{ km s}^{-1}$, *i.e.*, $N_{dark} \sim 182 \pm 40$ dark halos. Within a distance of 200 kpc we estimate $N_{dark} \approx 36 \pm 8$ for the Via Lactea and $N_{dark} \approx 91 \pm 20$ for the Aquarius simulation.

If the number of observed dwarf satellites within the Milky Way (after applying completeness corrections) is larger than N_{dark} we must conclude that some satellites are fossils. Twelve new ultra-faint dwarfs have been discovered around the Milky Way by analyzing SDSS data in a region that covers about 1/5 of the sky. Applying a simple correction for the sky coverage we estimate that there should be about at least 85 ± 14 Milky Way satellites. However, the data becomes incomplete for ultra-faint dwarf that are further than about 200 kpc from the Galactic center. Comparing this number of luminous satellites to N_{dark} within 200 kpc we cannot conclusively conclude that some ultra-faint dwarfs are fossils because N_{dark} for the Aquarius simulation is comparable to the estimate number of luminous satellites.

Once both sensitivity and survey area corrections are applied, Tollerud et al. (2008) estimates the existence of 300 to 600 luminous satellites within the virial radius ($R_{vir} \sim 400 \text{ kpc}$) of the Milky Way and 120 within 200 kpc. Comparing N_{dark} to the Tollerud et al. (2008) estimates of the number of luminous Milky Way satellites implies that a significant fraction of them are fossils (regardless if we use the Via Lactea or the Aquarius simulations estimates for N_{dark}). In Table 2.1 we have summarized the aforementioned results.

Another argument for the existence of fossils is provided by detailed comparison of the Galactocentric distribution of fossils in the Milky Way (GK06). Based on these comparison GK06 find that about 1/3 of Milky Way dwarfs may be fossils. In this paper, we show the GK06 theoretical results in comparison to updated observational data, including the new ultra-faint dwarfs found

using SDSS data, and applying completeness correction due to the limited area surveyed by the SDSS (about 1/5 of the sky). Assuming that the Local Group has a mass of $3 \times 10^{12} M_{\odot}$, as in the GK06 simulation, we find that there are no “missing galactic satellites” with $L_V \geq 10^5 L_{\odot}$ within the virial radius of the Milky Way. When the new dwarfs are included, the observed and predicted numbers of satellites agree near the Milky Way, however, for distances greater than 200 kpc, it is clear that there is still a ‘missing’ population of dwarfs. However, given that for $d > 200$ kpc, dwarfs with $L_V \sim 10^5 L_{\odot}$ drop below SDSS detection limits (Koposov et al, 2007), the under-abundance of observed dwarfs at large distances is not surprising and likely due to the SDSS sensitivity limit.

A final comment regards the cosmological model. The RG05 and GK06 simulations use cosmological parameters from WMAP 1. N-body simulations show that the number $N(M)$ of Milky Way dark matter satellites as a function of their mass is not overly sensitive to the cosmology, although there are some differences on the number of the most massive satellites (Madau et al. 2008). However, $N(v_{max})$ should be sensitive to the cosmology (Zentner & Bullock 2003), and changes of σ_8 and n_s may affect the occupation number and Galactocentric distribution of luminous halos. The collapse time of small mass halos in high density regions probably dominates the 20% variations in σ_8 between WMAP 1 and WMAP 3, limiting effects due to the cosmology near large halos. A decrease in luminous dwarf numbers, due to the lower σ_8 , could be evident in the distribution of the lowest mass luminous halos in the voids.

In conclusion, the number of Milky Way and M31 satellites provides an indirect test of galaxy formation and the importance of positive feedback in the early universe. Although the agreement of the SDSS and new M31 dwarfs’ properties with predictions from the RG05 and GK06 simulations does not prove the primordial origin of the new ultra-faint dwarfs, it supports this possibility with quantitative data and more successfully than any other proposed model has been able to do so far. At the moment, we do not have an ultimate observational test that can prove a dwarf galaxy to be a fossil. Even a test based on measuring the SFH of the dwarf galaxies may not be discriminatory because, as has been recently suggested, fossil galaxies may have a late phase of gas accretion and star formation at $z < 1 - 2$, during the last 9 – 10 Gyrs (Ricotti 2009). The distinction between fossils and non-fossils galaxies thus is quite tenuous and linked to our poor understanding of star formation and feedback in dwarf galaxies. Arguments based on counting the number of dwarfs in the Local Universe probably provide the most solid argument to prove or disprove the existence of fossil galaxies. In the future, a possible test may be provided by deep surveys looking for ultra-faint or dark galaxies in the local voids. Some fossil dwarfs should be present in the voids if they formed in large numbers before reionization.

REFERENCES

- Adelman-McCarthy, J. K., et al. 2007, ApJS, 172, 634
 Adelman-McCarthy, J. K., et al. 2006, ApJS, 162, 38

- Ahn, K., Shapiro, P. R., Alvarez, M. A., Iliev, I. T., Martel, H., & Ryu, D. 2006, *New Astronomy Review*, 50, 179
- Alvarez, M. A., Bromm, V., & Shapiro, P. R. 2006, *ApJ*, 639, 621
- Belokurov, V., et al. 2007, *ApJ*, 654, 897
- Belokurov, V., et al. 2006, *ApJ*, 647, L111
- Chapman, S. C., et al. 2007, *ApJ*, 662, L79
- Ciardi, B., Ferrara, A., & Abel, T. 2000, *ApJ*, 533, 594
- Ciardi, B., Scannapieco, E., Stoehr, F., Ferrara, A., Iliev, I. T., & Shapiro, P. R. 2006, *MNRAS*, 366, 689
- de Jong, J. T. A., et al. 2008, *ApJ*, 680, 1112
- Diemand, J., Kuhlen, M., & Madau, P. 2007, *ApJ*, 657, 262
- Geha, M., Willman, B., Simon, J. D., Strigari, L. E., Kirby, E. N., Law, D. R., & Strader, J. 2009, *ApJ*, 692, 1464
- Gnedin, N. Y. 2000, *ApJ*, 542, 535
- Gnedin, N. Y., & Kravtsov, A. V. 2006, *ApJ*, 645, 1054
- Haiman, Z., Abel, T., & Rees, M. J. 2000, *ApJ*, 534, 11
- Haiman, Z., Rees, M. J., & Loeb, A. 1996, *ApJ*, 467, 522
- Ibata, R., Martin, N. F., Irwin, M., Chapman, S., Ferguson, A. M. N., Lewis, G. F., & McConnachie, A. W. 2007, *ApJ*, 671, 1591
- Irwin, M. J., et al. 2007, *ApJ*, 656, L13
- Kirby, E. N., Simon, J. D., Geha, M., Guhathakurta, P., & Frebel, A. 2008, *ApJ*, 685, L43
- Klypin, A., Kravtsov, A. V., Valenzuela, O., & Prada, F. 1999, *ApJ*, 522, 82
- Koposov, S., et al. 2008, *ApJ*, 686, 279
- Kormendy, J., & Freeman, K. C. 2004, in *IAU Symposium*, 377
- Kravtsov, A. V., Gnedin, O. Y., & Klypin, A. A. 2004, *ApJ*, 609, 482
- Kroupa, P., Theis, C., & Boily, C. M. 2005, *A&A*, 431, 517
- Leitherer, C., et al. 1999, *ApJS*, 123, 3

- Machacek, M. E., Bryan, G. L., Meiksin, A., Anninos, P., Thayer, D., Norman, M., & Zhang, Y. 2000, *ApJ*, 532, 118
- Madau, P., Diemand, J., & Kuhlen, M. 2008, *ApJ*, 679, 1260
- Majewski, S. R., et al. 2007, *ApJ*, 670, L9
- Martin, N. F., Ibata, R. A., Chapman, S. C., Irwin, M., & Lewis, G. F. 2007, *MNRAS*, 380, 281
- Martin, N. F., Ibata, R. A., Irwin, M. J., Chapman, S., Lewis, G. F., Ferguson, A. M. N., Tanvir, N., & McConnachie, A. W. 2006, *MNRAS*, 371, 1983
- Mateo, M. L. 1998, *ARA&A*, 36, 435
- Mayer, L., Kazantzidis, S., Mastropietro, C., & Wadsley, J. 2007, *Nature*, 445, 738
- Mayer, L., Mastropietro, C., Wadsley, J., Stadel, J., & Moore, B. 2006, *MNRAS*, 369, 1021
- McConnachie, A. W., et al. 2008, *ApJ*, 688, 1009
- Moore, B., Ghigna, S., Governato, F., Lake, G., Quinn, T., Stadel, J., & Tozzi, P. 1999, *ApJ*, 524, L19
- Okamoto, T., Gao, L., & Theuns, T. 2008, *MNRAS*, 390, 920
- Peñarrubia, J., Navarro, J. F., & McConnachie, A. W. 2008, *ApJ*, 673, 226
- Ricotti, M. 2009, *MNRAS*, 392, L45
- Ricotti, M., & Gnedin, N. Y. 2005, *ApJ*, 629, 259
- Ricotti, M., Gnedin, N. Y., & Shull, J. M. 2001, *ApJ*, 560, 580
- Ricotti, M., Gnedin, N. Y., & Shull, J. M. 2002a, *ApJ*, 575, 33
- Ricotti, M., Gnedin, N. Y., & Shull, J. M. 2002b, *ApJ*, 575, 49
- Ricotti, M., Gnedin, N. Y., & Shull, J. M. 2008, *ApJ*, 685, 21
- Shapiro, P. R., & Kang, H. 1987, *ApJ*, 318, 32
- Simon, J. D., & Geha, M. 2007, *ApJ*, 670, 313
- Springel, V., et al. 2008, *MNRAS*, 391, 1685
- Stinson, G. S., Dalcanton, J. J., Quinn, T., Kaufmann, T., & Wadsley, J. 2007, *ApJ*, 667, 170
- Strigari, L. E., Bullock, J. S., Kaplinghat, M., Simon, J. D., Geha, M., Willman, B., & Walker, M. G. 2008, *Nature*, 454, 1096

- Tassis, K., Kravtsov, A. V., & Gnedin, N. Y. 2008, *ApJ*, 672, 888
- Tollerud, E. J., Bullock, J. S., Strigari, L. E., & Willman, B. 2008, *ApJ*, 688, 277
- Walsh, S. M., Jerjen, H., & Willman, B. 2007, *ApJ*, 662, L83
- Whalen, D., O’Shea, B. W., Smidt, J., & Norman, M. L. 2008, *ApJ*, 679, 925
- Willman, B., et al. 2005a, *AJ*, 129, 2692
- Willman, B., et al. 2005b, *ApJ*, 626, L85
- Zentner, A. R., & Bullock, J. S. 2003, *ApJ*, 598, 49
- Zentner, A. R., Kravtsov, A. V., Gnedin, O. Y., & Klypin, A. A. 2005, *ApJ*, 629, 219
- Zucker, D. B., et al. 2006a, *ApJ*, 650, L41
- Zucker, D. B., et al. 2006b, *ApJ*, 643, L103

Table 2. Summary of New Dwarfs Properties

Dwarf	Host	d_{hel} (d_{M31}) (kpc)	M_V (mag)	μ_o ($mag\ arcsec^{-2}$)	$r_{1/2}$ (pc)
Bootes I	MW	62 ± 3^a	-5.8 ± 0.5^f	28.3 ± 0.5^f	230^a
Bootes II	MW	60 ± 10^b	-3.1 ± 1.1^b	29.8 ± 0.8^b	72 ± 28^b
Canes Venatici I	MW	$220^{+25}_{-16}^c$	-7.9 ± 0.5^c	28.2 ± 0.5^c	550^c
Canes Venatici II	MW	$150^{+15}_{-14}^d$	-4.8 ± 0.6^d	-	$\sim 140^d$
Coma Berenics	MW	44 ± 4^d	-3.7 ± 0.6^d	-	70^d
Hercules	MW	$140^{+13}_{-12}^d$	-6.0 ± 0.6^d	-	$\sim 320^d$
Leo IV	MW	$160^{+15}_{-14}^d$	-5.1 ± 0.6^d	-	$\sim 160^d$
Leo T	MW	$\sim 420^e$	-7.1^e	26.9^e	$\sim 170^e$
Ursa Major I	MW	$106^{+9}_{-8}^g$	-5.6 ± 0.6^g	-	308 ± 32^g
Ursa Major II	MW	30 ± 5^a	-3.8 ± 0.6^h	-	127 ± 21^g
Segue I	MW	23 ± 2^n	$-1.5^{+0.6}_{-0.8}^n$	-	29 ± 8^n
Willman I	MW	38 ± 7^i	-2.5 ± 1.0^i	-	21 ± 5^i
And XI	M31	$\sim 770^j$	-7.3 ± 0.5^j	-	115 ± 45^j
And XII	M31	$830 \pm 50 (\sim 105)^k$	-6.9^k	-	137^k
And XIII	M31	$\sim 770^j$	-6.9 ± 1.0^j	-	115 ± 45^j
And XIV	M31	871^m	-	-	-
And XV	M31	$630 \pm 60 (170)^l$	-9.4^l	-	-
And XVI	M31	$525 \pm 50 (270)^l$	-9.2^l	-	-

^aMartin et al. (2007)

^bWalsh et al. (2007)

^cZucker et al. (2006b)

^dBelokurov et al. (2007)

^eIrwin et al. (2007)

^fBelokurov et al. (2006)

^gSimon & Geha (2007)

^hZucker et al. (2006a)

ⁱWillman et al. (2005a)

^jMartin et al. (2006)

^kChapman et al. (2007)

^lIbata et al. (2007)

^mMajewski et al. (2007)

ⁿGeha et al. (2009)

Table 3. Summary of New Dwarfs Properties cont.

Dwarf	Host	Type	[Fe/H]	σ ($km s^{-1}$)	M_{TOT} ($10^6 M_{\odot}$)	M/L
Bootes I	MW	dSph	-2.1 ^a	$6.5^{+2.0}_{-1.4}$ ^a	13 ^a	~ 700 ^a
Bootes II	MW	dSph	-2.0 ^c	-	-	-
Canes Venatici I	MW	dSph	-2.09 ± 0.02 ^b	7.6 ± 0.4 ^b	27 ± 4 ^b	221 ± 108 ^b
Canes Venatici II	MW	dSph	-2.31 ± 0.12 ^b	4.6 ± 1.0 ^b	2.4 ± 1.1 ^b	336 ± 240 ^b
Coma Berenics	MW	dSph	-2.0 ± 0.07 ^b	4.6 ± 0.8 ^b	1.2 ± 0.4 ^b	448 ± 297 ^b
Hercules	MW	dSph	-2.27 ± 0.07 ^b	5.1 ± 0.9 ^b	7.1 ± 2.6 ^b	332 ± 221 ^b
Leo IV	MW	dSph	-2.31 ± 0.1 ^b	3.3 ± 1.7 ^b	1.4 ± 1.5 ^b	151 ± 177 ^b
Leo T	MW	dSph/dIrr	-2.29 ± 0.1 ^b	7.5 ± 1.6 ^b	8.2 ± 3.6 ^b	138 ± 71 ^b
Ursa Major I	MW	dSph	-2.06 ± 0.1 ^b	7.6 ± 1.0 ^b	15 ± 4 ^b	1024 ± 636 ^b
Ursa Major II	MW	-	-1.97 ± 0.15 ^b	6.7 ± 1.4 ^b	4.9 ± 2.2 ^b	1722 ± 1226 ^b
Segue I	MW	dSph	-2.8 ± 0.2 ^g	4.3 ± 1.2 ^g	$0.45^{+4.7}_{-2.5}$ ^g	1320^{+2680}_{-940} ^g
Willman I	MW	dSph	-1.5 ^a	$4.3^{+2.3}_{-1.3}$ ^a	0.5 ^a	~ 470 ^a
And XI	M31	-	-1.3 ± 0.5 ^d	-	-	-
And XII	M31	dSph	-1.5 ± 0.4 ^d	-	-	-
And XIII	M31	-	-1.4 ± 0.5 ^d	-	-	-
And XIV	M31	dSph	-1.7 ^e	6.2 ± 1.3 ^e	33^{+31}_{-8} ^e	165^{+156}_{-92} ^e
And XV	M31	-	-1.1 ^f	-	-	-
And XVI	M31	-	-1.7 ^f	-	-	-

^aMartin et al. (2007)

^bSimon & Geha (2007)

^cWalsh et al. (2007)

^dMartin et al. (2006)

^eMajewski et al. (2007)

^fIbata et al. (2007)

^gGeha et al. (2009)